Applied Catalysis B: Environmental 253 (2019) 105–110

Contents lists available at ScienceDirect

Applied Catalysis B: Environmental

journal homepage: www.elsevier.com/locate/apcatb

Sensitizing Ru(II) polyimine redox center with strong light-harvesting coumarin antennas to mimic energy flow of biological model for efficient hydrogen evolution

Nan Zhang[a], Kai-Kai Chen[a], Song Guo[a,*], Ping Wang[a], Min Zhang[a], Jianzhang Zhao[b], Zhi-Ming Zhang[a,*], Tong-Bu Lu[a]

[a] Institute for New Energy Materials and Low Carbon Technologies, School of Material Science & Engineering, Tianjin University of Technology, Tianjin 300384, PR China
[b] State Key Laboratory of Fine Chemicals, School of Chemical Engineering, Dalian University of Technology, Dalian 116024 China

ARTICLE INFO

Keywords:
Hydrogen evolution
Ru-based photosensitizer
Strong visible light absorption
Energy transfer

ABSTRACT

In natural photosynthetic system, sunlight is trapped by strongly absorbing chromophores, followed by excitation energy transfer to redox centers to initiate redox reactions. This inspired chemists to decorate redox centers with antenna molecules to mimick energy flow of biological model. Herein, three strong light-harvesting coumarin antennas were firstly decorated to a Ru(II) complex, resulting in a tetrads (**Ru-3**) with high molar extinction coefficient of 144000 $M^{-1} cm^{-1}$ at 481 nm, 13-fold higher than that of typical $Ru(bpy)_3^{2+}$ (bpy = 2,2′-bipyridine, **Ru-1**). Photocatalytic hydrogen evolution activity of **Ru-3** is over 27 times higher than that of **Ru-1** under weak visible-light condition, while achieving a turnover number (TON) of 5510 under 175 W Xenon lamp irradiation. Steady and transient spectra confirm that the strong absorbing coumarins are responsible for capturing visible light and subsequently funneling the excitation energy to Ru redox center, which can efficiently promote the electron transfer from *N*, *N*-dimethyl-*p*-toluidine (**DMT**) to excited redox center, as well as the subsequent photocatalytic hydrogen evolution.

1. Introduction

Visible light-driven water splitting into hydrogen has been regarded as a promising method to utilize sustainable sun light and earth-abundant raw materials (H_2O) to produce renewable and clean H_2 fuel [1–7].Therefore, many efforts have been devoted to exploring efficient systems for photocatalytic hydrogen evolution [8–17].As well known, efficient photosynthetic system requires not only a strong light-harvesting photosensitizer (PS), but also the efficient electron and energy transfer between different components [18–20].PS, as the light-harvesting body and electron transfer mediator between catalyst and electron donor, has become limiting component of the whole system [21].At present, **Ru-1**, as one of the most widely used PSs, was frequently used as both the chromophore and redox center [22–25],but it possesses of humble absorptivity ($\varepsilon < 16000\ M^{-1} cm^{-1}$) in the visible region, which usually frustrated its efficiency as a PS in the context of hydrogen evolution [20,24,26–29].Against this drawback, organic chromophore-decorating PSs has been proved to be an efficient strategy to enhance the molar absorptivity for efficient H_2 evolution [30].However, for Ru(II)-based complexes with strong visible-light-absorbing antennas, the reduction potential usually becomes more positive, resulting in limited choice of water splitting catalysts [21].Accordingly, it is still a great challenging task to dramatically improve water splitting ability by only enhancing the visible light absorbability of the PSs [31].In the biological systems, the photosynthetic process displays a cooperative manner between light absorption and redox reaction, where the strongly absorbing antennas, such as chlorophyll b, absorb the visible light and then transfer the excitation energy to the redox center of chlorophyll *a* to drive water oxidation and $NADP^+$ reduction at different stages (Scheme 1) [32–35].Accordingly, coupling intense visible-light-harvesting antennas with redox centers to mimic energy flow of biological model can supply an efficient way to construct efficient artificial photosynthetic system for energy conversion [36].

Inspired by photosynthetic organisms, we design and synthesize two Ru(II)-coumarin complexes (**Ru-2** and **Ru-3**) with much stronger visible-light-harvesting ability than that of **Ru-1** (Scheme 2, Figs. S1–S9). Remarkably, **Ru-3**, with three coumarin antennas, shows an intense absorption band between 400–550 nm Figs. 1a and S10) with a molar extinction coefficient of 144000 $M^{-1} cm^{-1}$ at 481 nm,13 times higher than that of **Ru-1** (11400 $M^{-1} cm^{-1}$ at 450 nm). It is noteworthy

* Corresponding authors.
E-mail addresses: guosong@email.tjut.edu.cn (S. Guo), zmzhang@email.tjut.edu.cn (Z.-M. Zhang).

https://doi.org/10.1016/j.apcatb.2019.04.039
Received 18 February 2019; Received in revised form 8 April 2019; Accepted 14 April 2019
Available online 15 April 2019
0926-3373/

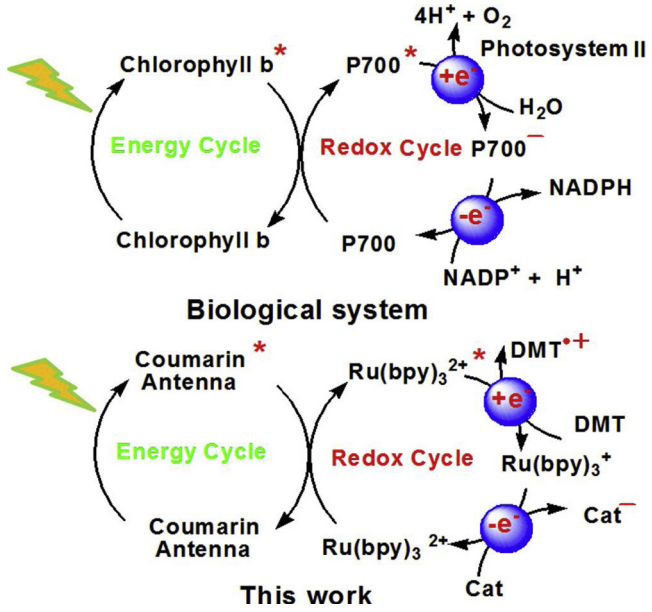

Scheme 1. Biological photosynthetic system (top), and electronic excitation energy transfer in the photoredox processes for hydrogen evolution (bottom).

that the reduction potential of **Ru-3** is −1.36 V, even more negative than that of **Ru-1** (−1.33 V) after the decoration of coumarin, which is beneficial for enlarging the selection range of water splitting catalysts with strong visible-light absorption antennas. Steady and transient spectra demonstrate that the light is initially captured by coumarin antennas, which can be efficiently converted into triplet excited state by the cascade intramolecular photophysical processes. The dramatically enhanced visible light absorption ability and efficient excitation energy conversion result in high-performance photocatalytic hydrogen evolution.

2. Experimental section

2.1. Materials and methods

All the reactions were performed in argon unless otherwise mentioned. All the solvents were analytical grade and distilled before use. The $RuCl_3 \cdot 3H_2O$, 1,10-Phenanthroline and 2,2-bipyridine were purchased from Sigma-Aldrich. The 7-(diethylamino) coumarin-3-carbaldehyde, NH_4PF_6 and ethylene glycol were purchased from Alfa Aesar. Chromatographic grade acetonitrile was purchased from Adamas Reagent. The synthetic scheme of **Ru-2** and **Ru-3** is presented in Scheme S1. The synthetic intermediates and target complexes were characterized by ^{1}H NMR and EI mass spectroscopy.

2.2. Instruments

^{1}H NMR spectra were recorded with a AVANCE III HD 400 MHz. High resolution mass spectra were performed on Q-TOF LC–MS with an ESI mode. Electrochemical tests were performed on a CHI 760E electrochemical workstation. The yield of hydrogen was detected by gas chromatography (Shimadzu GC-2014 + AT 230C, TDX-01 column, TCD, argon carrier). UV–vis absorption spectra of all the compounds taken on a LAMBDA750 UV–vis spectrophotometer. Fluorescence spectra were recorded on Hitachi F4500 spectrofluorometer. Transient absorption spectra were monitored by LP980 laser flash photolysis instrument (Edinburgh, U.K.). Photocatalytic experiments were conducted with a 470 nm LED light (Zolix, MLED4) and 175 W Xenon lamp (LX-175, PEILC, Japan) with 420 nm filter.

2.3. Visible light-driven hydrogen production

Photocatalytic experiments were carried out under 1 atm of Ar in 16 m L reactor containing complexes PS (5.0 μM), **C-1** (77.5 μM), **DMT** (5.3 mM), H_2O (0.56 M) and 3 m L CH_3CN. The mixture was continuously stirred and irradiated under a blue LED light (λ = 470 nm, 120 mW cm^{-2}, irradiation area of 0.8 cm^2). Xenon lamp as a bandbroad light source also was used for photocatalytic hydrogen evolution and its power was determined as 200 mW cm^{-2}.

2.4. Spectrum measurement

Chromatographic pure reagents were used for spectra tests, and all the measurements were conducted under 1 atm argon atmosphere unless otherwise stated. For the accuracy of the test results, $Ru(bpy)_3^{2+}$ was selected as a reference material to check the apparatus and the method of measurement.

3. Results and discussion

Ru-2 and **Ru-3** were both synthesized by a two-step method with yields of over 65%. In this synthetic process, $Ru(bpy)_2Cl_2$ and $Ru(DMSO)_4Cl_2$ were prepared according to previous reported methods and used as the precursors to react with coumarin ligand (**L-1**) to synthesize the target products **Ru-2** and **Ru-3** (Figs. S1–S9) [37,38].

In order to investigate the energy transfer process from antennas to redox centers, the emission spectra of **L-1**, **Ru-2** and **Ru-3** were compared. As shown in Fig. 1b, the coumarin ligand (**L-1**) showed a strong fluorescence peak at 500 nm upon excitation at 450 nm. Upon excitation of the coumarin antenna, the phosphorescence of Ru coordination center at 593 nm for **Ru-2** and 587 nm for **Ru-3** were observed, and no emission peak around 500 nm of coumarin antenna was detected, indicating efficient energy transfer from coumarin antennas to Ru coordination center [39,40].This was further comfirmed by superimposable absorption and excitation spectra of **Ru-2** and **Ru-3** (Figs. S11 and S12) [36].Furthermore, **Ru-3** shows a stronger phosphorescence intensity than that of **Ru-2** under the same condition, indicating more efficient light-harvesting ability of **Ru-3** than that of the monocoumarin-decorating **Ru-2**. Otherwise, the photophysical process of direct ^{1}IL→^{3}IL transition has usually considered as a possible pathway to quench the fluorescence of coumarin antenna. However, in this work, the far distance between Ru(II) center and coumarin antenna can dramatically reduce the heavy atom effect. Additionally, the efficient energy transfer from Coumarin to Ru center has also been confirmed by both comparison of absorption and excitation spectra of **Ru-3** (Fig. S11), and the emission spectra of **L-1** and **Ru-3** under the same condition (Fig. 1b). It can be concluded that intersystem crossing (ISC) process was inefficient in quenching the fluoresence of coumarin molecules.

Further, we introduced **DMT** and **C-1** into the **Ru-2** – **Ru-3**-containing biomimetic systems to evaluate their electron transfer efficiency and photocatalytic hydrogen evolution ability (Figs. 2, S13 and S14, Table S1). Under the irradiation of 470 nm LED light, their photocatalytic activity was in the order of **Ru-3** > **Ru-2** > **Ru-1** (Fig. 2a). Various control experiments were further performed, no or trace amount of H_2 was detected in the absence of **Ru-1** – **Ru-3**, **C-1**, **DMT**, or water, confirming that all above factors were necessary for hydrogen production. In addition, no H_2 evolved with isolated coumarin (**L-1**) as PS, manifesting that the isolated coumarin antenna can not drive water splitting into hydrogen, although it possesses of strong visible light-harvesting ability. The key function of coumarin antenna is to harvest light and funnel the captured light energy to redox center (Fig. 2a). These results preliminarily support that this is a feasible strategy to decorate redox center with strongly absorbing chromophores.

To directly compare the effect of the light harvesting ability on the photocatalytic performance, the photocatalytic experiments of **Ru-1**–

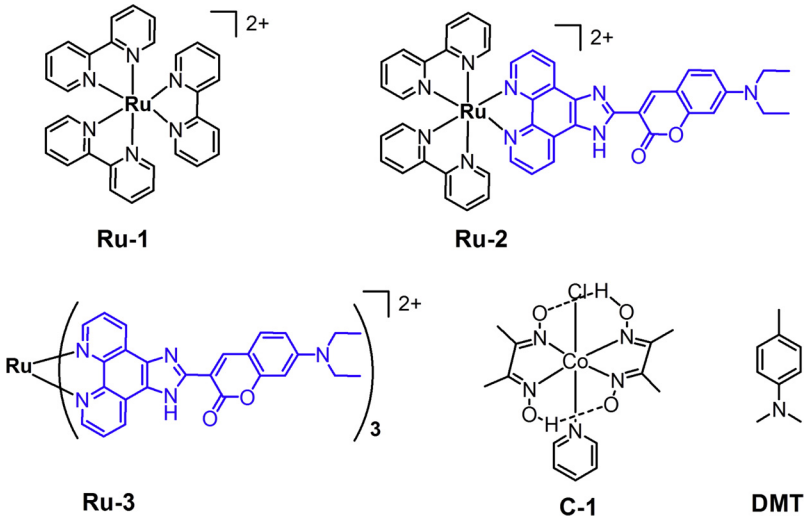

Scheme 2. The structures of **Ru-1** – **Ru-3**, **C-1** and **DMT**.

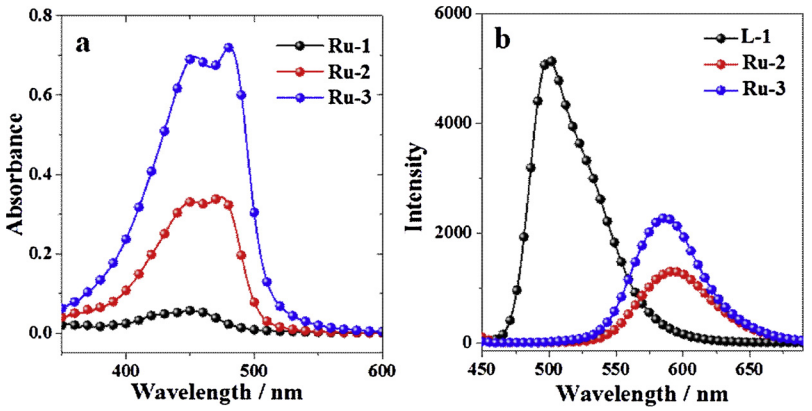

Fig. 1. a) UV–vis absorption spectra of **Ru-1** – **Ru-3** with a same concentration; b) Comparison of emission of **L-1**, **Ru-2**, and **Ru-3** under the same condition, λ_{ex} = 450 nm, c = 5.0 μM in CH_3CN.

and **Ru-3**–containing systems were carried out under different light intensity (Figs. 2b and c and S15). As shown in Fig. 2b, the photocatalytic activity of **Ru-1** significantly decreased with weakening the light intensity. For comparsion, much less fluctuation of the catalytic performance of **Ru-3** was detected under different light intensity. Remarkably, under the radiated power of 44 mW/cm^2, TON of **Ru-3** is still up to 459, 27 times higher than that of **Ru-1** (17), and the TON of **Ru-2** (258) is 15 times higher than that of **Ru-1** (Fig. 2c). Under the same condition, the photocatalytic performance of **Ru-1**-containing system was not improved by addition of coumarin molecules (Fig. 2c), indicating that light energy, absorbed by L-**1**, cannot be efficiently transferred to Ru redox center due to the far distance between **Ru-1** and **L-1** (Fig. 2c). All these results demonstrate that covalently decorating the redox centers with coumarin molecules could efficiently promote the electronic excitation energy transfer from antenna to the redox centers to efficiently drive the redox reactions. This also represents the first Ru(II) complexes with intense visible light harvesting antennas used for photocatalytic hydrogen production. In addition, considering that **Ru-3** displayed a bandbroad absorption between 400–550 nm, the photocatalytic experiment was further performed under 175 W Xenon lamp in the visible region (Fig. 2d), and TON toward **Ru-3** was up to 5510 at μM concentration of **Ru-3**. When the concentration of **Ru-3** increased from 1 μM to 10 μM, the amount of hydrogen production also increased from 17 μmol to 50 μmol, indicating an efficient photocatalytic system for hydrogen production.

In order to study the efficiency of electron transfer, phosphorescence quenching experiments of **Ru-1** – **Ru-3** were carried out by varying the concentrations of **DMT** and **C-1**, respectively. Sternvolmer quenching constants of **Ru-3** and **Ru-2** by **DMT** were up to 1.4×10^4 M^{-1} and 8.5×10^3 M^{-1}, ca. 22-fold and 13-fold higher than that of **Ru-1** (6.4×10^2 M^{-1}), respectively (Figs. 3b and S13). These results indicated that the excited Ru coordination center in **Ru-2** and **Ru-3** could more efficiently accept electron from **DMT** than **Ru-1**. Similarly, the phosphorescence of **Ru-1** – **Ru-3** can be also efficiently quenched by **C-1** (Fig. S14). Nevertheless, the photocatalytic pathway should be determined as the reductive quenching mechanism, as the concentration of **DMT** (5.3 mM) is much higher than that of **C-1** (0.078 mM) in the photocatalytic system [41].In this process, the excited Ru-based complexes firstly accepted an electron from **DMT** to produce reduced Ru-based species, which can further reduce Co(III) to Co(I) via a multi-electron transfer process. This process was also systematically verified by transient absorption spectra (Figs. 3, S16-S18).

Nanosecond transient absorption spectra were performed to unveil electron transfer processes between redox centers and **DMT**/ **C-1** (Figs. 3, S16–S18). As a typical ^{3}MLCT complex, **Ru-1** shows a ground state bleaching peak around 450 nm and a positive peak around 380 nm (Fig. S16a). As shown in Fig. S16b, a long-lived positive peak around 500 nm could be assigned to the absorption of reduced **Ru-1** in the presence of **DMT** [42,43].**Ru-2** and **Ru-3** show a similar transient spectra, which display a dual bleaching peak around 460 nm and a positive absorption band between 500 nm and 600 nm, supporting that an equilibrium state between ^{3}MLCT and ^{3}IL excited states was

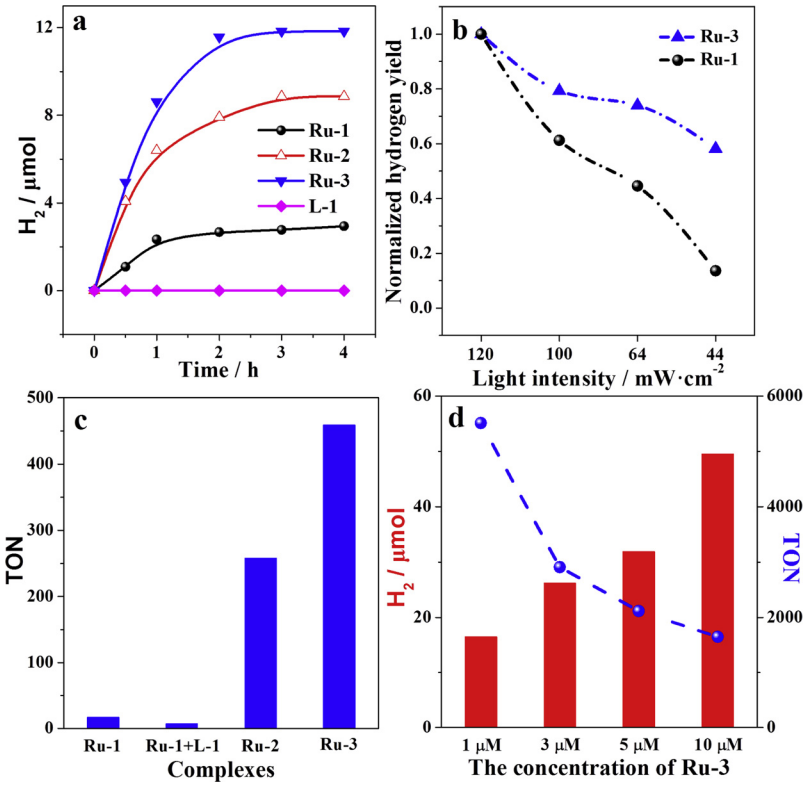

Fig. 2. Photocatalytic hydrogen evolution with irradiation of a) 470 nm LED with light intensity of 120 mW/cm^2; b) 470 nm LED with different light intensity; c) 470 nm LED with light intensity of 44 mW/cm^2; d) 175 W xenon light with a 420 nm filter (light intensity: 200 mW/cm^2. Photocatalytic conditions: a–c) 5.0 μM PSs, 77.5 μM **C-1**, and 5.3 mM **DMT**, d) 155.0 μM **C-1**, and 60.0 mM **DMT** in CH_3CN/H_2O.

populated upon 430 nm excitation (Figs. 3a and S17a) [36].Furthermore, **Ru-2** gave a negative band at 600–650 nm, which could be tentatively attributed to its background phosphorescence. After addition of **DMT**, a new sharp positive peak around 512 nm and a bleaching peak around 478 nm were detected with a long-lived decay for both **Ru-2** and **Ru-3**, which could be attributed to the reduced **Ru-2** and **Ru-3** (Fig. 3c and S17b). This was also proved by emission quenching experiments, showing an efficient electron transfer from **DMT** to excited Ru-based complexes (Fig. 3b). Further, the transient spectra of reduced **Ru-2** and **Ru-3** with **C-1** were similar to that of native **Ru-2** and **Ru-3**, indicating that the reduced **Ru-2** and **Ru-3** can rapidly transfer electrons to **C-1** to return to their ground state and yielding Co^{2+}/Co^{+} species (Fig. 3e) [41].

Notably, under the same condition, the ΔOD value (quantificationally represents the excited state absorption ability) of **Ru-2** and **Ru-3** is much larger than that of **Ru-1** at the delay time of 0 μs upon 450 nm excitation (Fig. 3f) [44].The order of ΔOD values is **Ru-3** > **Ru-2** > **Ru-1**, in agreement with their visible light-harvesting ability with the same concentration. As well known, the ΔOD value is proportional to the concentration of excited state PSs. The amounts of the transient

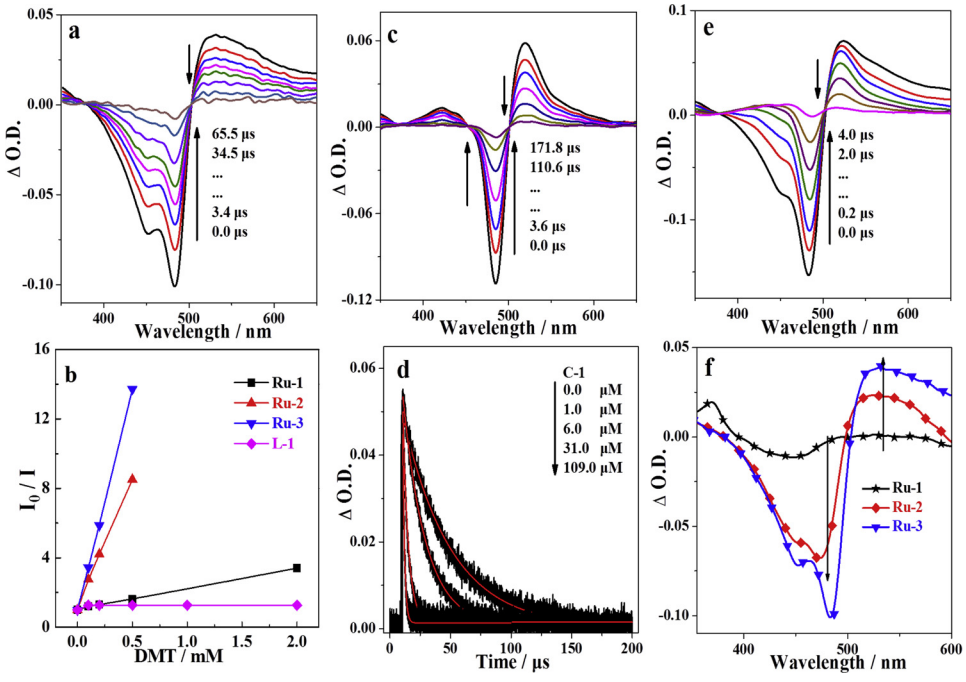

Fig. 3. Nanosecond transient absorption spectra of a) **Ru-3**; b) Stern-Volmer plots of **L-1**, and **Ru-1** – **Ru-3**, obtained by steady emission quenching experiment; c) **Ru-3** with 5.3 mM **DMT**; d) Kinetic traces of reduced **Ru-3** with different concentration of **C-1** followed at 510 nm; e) **Ru-3** with 5.3 mM **DMT** and 0.1 mM **C-1**; f) comparison of transient absorption spectra of **Ru-1** – **Ru-3** with delay time of 0 μs under the same condition; Conditions: 5.0×10^{-6} M **Ru-1** – **Ru-3** under N_2 atmosphere in CH_3CN.

Table 1
Summary of the photophysical data of **Ru-1** – **Ru-3**[a].

	λ/nm	ε/(M^{-1}·cm^{-1})	τ_T/μs[b]	τ_T/μs[c]	$K_1/(M^{-1})$[d]	$K_2/(M^{-1})$[e]	$K_3/(M^{-1})$[f]
Ru-1	450	11400	0.8	99.4	6.4×10^2	1.8×10^5	9.8×10^2
Ru-2	474	68600	8.2	133.9	8.5×10^3	8.0×10^5	9.0×10^3
Ru-3	481	144000	14.7	50.0	1.4×10^4	3.0×10^5	3.6×10^4

[a] 5.0 μM **Ru-1** – **Ru-3**, 77.5 μM **C-1**, and 5.3 mM **DMT** in CH_3CN/H_2O.
[b] Triplet excited state lifetime measured by transient absorption.
[c] Lifetime of reduced **Ru-1** – **Ru-3**. Stern-Volmer quenching constant of.
[d] **Ru-1** – **Ru-3** with **DMT** as the quencher.
[e] reduced **Ru-1** – **Ru-3** quenched by **C-1**.
[f] **Ru-1** – **Ru-3** with **C-1** as the quencher.

species were calculated from the transient absorption spectra according to their molar absorption coefficients. As a result, the concentrations of the transient species were determined to be in the order of **Ru-3** (4.29×10^{-7} M) > **Ru-2** (2.16×10^{-7} M) > **Ru-1** (4.25×10^{-8} M) (the detail calculated method was supplied in the supporting information).Therefore, it could be concluded that the captured light energy by coumarin antenna of **Ru-3** and **Ru-2** can be efficiently converted into their triplet states, which further promoted the electron transfer from **DMT** to the exited state complexes (**Ru-3** and **Ru-2**).

The dynamics processes of **Ru-1** – **Ru-3** with **DMT** and **C-1** were also performed to further clarify the electron transfer efficiency from reduced redox center to **C-1**. Their reduced state, e.g. **Ru-3**, could be efficiently oxidized by **C-1** with a constant of 3.0×10^5 M^{-1}, indicating an efficient electron transfer from reduced **Ru-3** to **C-1** (Fig. 3e and Table 1). The reduced **Ru-1** and **Ru-2** can also efficiently transfer electrons to **C-1**, and their stern-volmer constants were determined as 1.8×10^5 M^{-1} and 8.0×10^5 M^{-1}, respectively (Table 1). And the second order rate constants of reduced **Ru-1** – **Ru-3** by **C-1** were determined as 2.8×10^9 $M^{-1}s^{-1}$, 6.0×10^9 $M^{-1}s^{-1}$ and 5.9×10^9 $M^{-1}s^{-1}$, respectively, which were very close to the diffusion-controlled limits (~10^{10} $M^{-1}s^{-1}$) (Fig. S19, Table S2). Most of all, kinetic constants of reduced **Ru-2** and **Ru-3** were much superior to that of reduced **Ru-1**, supporting that coupling of antenna molecules to Ru redox center can efficiently promote the electron transfer from reduced redox center to **C-1**.

The lifetimes of excited state and reduced state of these complexes were also detected (Fig. 3 and Table 1). The excited lifetimes of **Ru-3** and **Ru-2** were determined as 14.7 μs and 8.2 μs, much longer than that of **Ru-1** (0.8 μs), which could be ascribed to the equilibrium between ^{3}MLCT and ^{3}IL state in both **Ru-3** and **Ru-2** [36].The long-lived excited states of these coumarin antenna-decorating complexes can supply more enough time for electron transfer from **DMT** to these exited state Ru-based complexes [21].In addition, all these complexes have a long-lived reduced state (Table 1), which contributes to the efficient electron transfer from reduced **Ru-1** – **Ru-3** to the catalytically active center.

Thermodynamic feasibility of electron transfer among three components were studied by electrochemical method (Table S3) [45,46]. As shown in Fig. 4, the oxidation potential of **DMT** is more negative than the reduction potential of excited state **Ru-1** – **Ru-3**, and the reduction potential of **Ru-1** – **Ru-3** is more negative than that of both Co^{3+}/Co^{2+} and Co^{2+}/Co^{+}. Furthermore, the oxidation potential of excited state **Ru-1** is higher than the reduction potential of Co^{3+}/Co^{2+}, but lower than that of Co^{2+}/Co^{+}, excluding the oxidation quenching mechanism for **Ru-1**. Hence, all these results further confirmed that the photocatalytic process could be attributed to reductive quenching mechanism.

Based on all above results, photoredox cycle of **Ru-2** and **Ru-3**-based photocatalytic system was illuminated in Scheme 3. Upon photoexcitation, the light was absorbed by strongly absorbing coumarin antennas, followed by the fast electronic excitation energy transfer to the redox centers and then transformation into triplet state by a series of intramolecular photophysical processes. Afterward, the triplet state

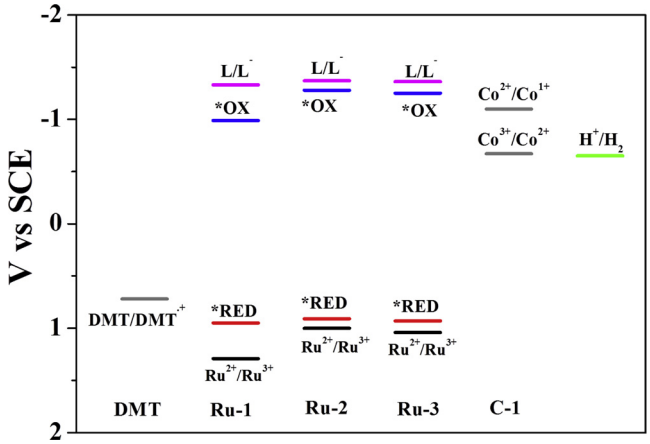

Fig. 4. Energy diagram depicting the redox potentials of relevant species present in the catalytic system. *Ox and *Red represent excited state oxidation and reduction potentials, respectively. (For interpretation of the references to colour in this figure legend, the reader is referred to the web version of this article).

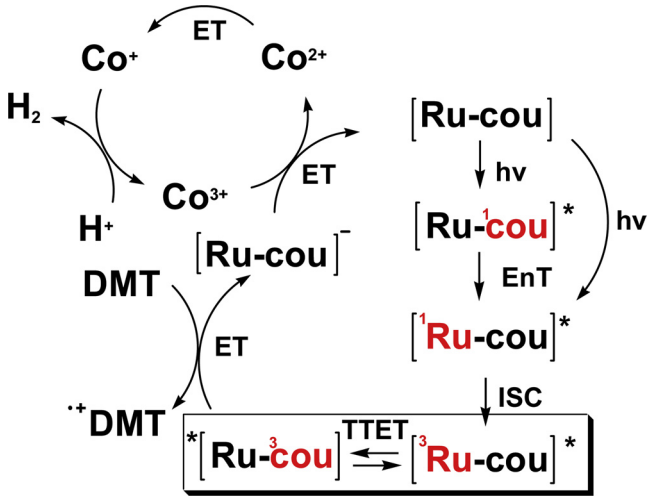

Scheme 3. Proposed energy and electron transfer process and photoredox cycle for visible-light induced hydrogen evolution with **Ru-cou** (**Ru-2** and **Ru-3**). Ru is the coordination center, cou is coumarin antenna, EnT is energy transfer, ET is electron transfer, ISC is intersystem crossing, TTET stands for triplet-triplet energy transfer.

of **Ru-2** (or **Ru-3**) accepted an electron from **DMT** to produce the reduced **Ru-2** (or **Ru-3**), which could consecutively donor two electrons to reduce Co^{3+} to Co^{+}. It could be obviously observed that sensitizing Ru(II) polyimine redox center with antennas can dramatically enhance the conversion of visible-light into redox energy by mimicking the energy flow of biological model. Ultimately, the resulting Co^{+} species were used to reduce protons for efficient hydrogen evolution.

4. Conclusions

In conclusion, the strongly absorbing coumarin antennas of **Ru-2** and **Ru-3**, only composed of earth abundant C, H, O and N elements, can efficiently funnel excitation energy to Ru(II) polyimine redox center to promote the electron transfer from **DMT** to excited redox center and further boost hydrogen production. The photocatalytic performance of **Ru-3** is over 27 times higher than that of typical **Ru-1** under weak visible-light irradiation. Thus, the described biological mimic method not only dramatically improves photocatalytic performance for producing clean fuel, but also enables inactive pigments as efficient light-harvesting molecules for water splitting.

Conflicts of interest

The authors have no conflicts to declare.

Acknowledgments

This work was supported by National Key R&D Program of China (2017YFA0700104) and the National Natural Science Foundation of China (Nos. 21703155, 21722104, 21671032,21401095), Natural Science Foundation of Tianjin City of China (18JCQNJC76500) (18JCJQJC47700, 17JCQNJC05100), Natural Science Foundation for Distinguished Young Scholars of Tianjin of China (17JCJQJC43800).

Appendix A. Supplementary data

Supplementary material related to this article can be found, in the online version, at doi:https://doi.org/10.1016/j.apcatb.2019.04.039.

References

[1] Y.J. Yuan, Z.T. Yu, D.Q. Chen, Z.G. Zou, Chem. Soc. Rev. 46 (2017) 603–631.
[2] K.L. Mulfort, L.M. Utschig, Acc. Chem. Res. 49 (2016) 835–843.
[3] M. Wang, K. Han, S. Zhang, L. Sun, Coord. Chem. Rev. 287 (2015) 1–14.
[4] T.S. Teets, D.G. Nocera, Chem. Commun. 47 (2011) 9268–9274.
[5] P. Du, R. Eisenberg, Energy Environ. Sci. 5 (2012) 6012.
[6] Z. Han, R. Eisenberg, Acc. Chem. Res. 47 (2014) 2537–2544.
[7] N. Kaeffer, M. Chavarot-Kerlidou, V. Artero, Acc. Chem. Res. 48 (2015) 1286–1295.
[8] S. Yang, B. Pattengale, S. Lee, J. Huang, ACS Energy Lett. 3 (2018) 532–539.
[9] M. Liu, Y.-F. Mu, S. Yao, S. Guo, X.-W. Guo, Z.-M. Zhang, T.-B. Lu, Appl. Catal. B: Environ. 245 (2019) 496–501.
[10] X.B. Li, Y.J. Gao, Y. Wang, F. Zhan, X.Y. Zhang, Q.Y. Kong, N.J. Zhao, Q. Guo, H.L. Wu, Z.J. Li, Y. Tao, J.P. Zhang, B. Chen, C.H. Tung, L.Z. Wu, J. Am. Chem. Soc. 139 (2017) 4789–4796.
[11] Z. Han, W.R. McNamara, M.S. Eum, P.L. Holland, R. Eisenberg, Angew. Chem. Int. Ed. 51 (2012) 1667–1670.
[12] O. Schott, A.K. Pal, D. Chartrand, G.S. Hanan, ChemSusChem 10 (2017) 4436–4441.
[13] B.S. Veldkamp, W.-S. Han, S.M. Dyar, S.W. Eaton, M.A. Ratner, M.R. Wasielewski, Energy Environ. Sci. 6 (2013) 1917.
[14] J.I. Goldsmith, W.R. Hudson, M.S. Lowry, T.H. Anderson, S. Bernhard, J. Am. Chem. Soc. 127 (2005) 7502–7510.
[15] R.S. Khnayzer, C.E. McCusker, B.S. Olaiya, F.N. Castellano, J. Am. Chem. Soc. 135 (2013) 14068–14070.
[16] J.-X. Jian, C. Ye, X.-Z. Wang, M. Wen, Z.-J. Li, X.-B. Li, B. Chen, C.-H. Tung, L.-Z. Wu, Energy Environ. Sci. 9 (2016) 2083–2089.
[17] Z.M. Zhang, T. Zhang, C. Wang, Z. Lin, L.S. Long, W. Lin, J. Am. Chem. Soc. 137 (2015) 3197–3200.
[18] J. Zhao, W. Wu, J. Sun, S. Guo, Chem. Soc. Rev. 42 (2013) 5323–5351.
[19] G. Li, M.F. Mark, H. Lv, D.W. McCamant, R. Eisenberg, J. Am. Chem. Soc. 140 (2018) 2575–2586.
[20] A. Fihri, V. Artero, M. Razavet, C. Baffert, W. Leibl, M. Fontecave, Angew. Chem. Int. Ed. 120 (2008) 574–577.
[21] S. Guo, K.-K. Chen, R. Dong, Z.-M. Zhang, J. Zhao, T.-B. Lu, ACS Catal. 8 (2018) 8659–8670.
[22] D. Streich, Y. Astuti, M. Orlandi, L. Schwartz, R. Lomoth, L. Hammarstrom, S. Ott, Chem. Eur. J. 16 (2010) 60–63.
[23] M. Natali, ACS Catal. 7 (2017) 1330–1339.
[24] W.R. McNamara, Z. Han, C.J. Yin, W.W. Brennessel, P.L. Holland, R. Eisenberg, Proc. Natl. Acad. Sci. U. S. A. 109 (2012) 15594–15599.
[25] W.R. McNamara, Z. Han, P.J. Alperin, W.W. Brennessel, P.L. Holland, R. Eisenberg, J. Am. Chem. Soc. 133 (2011) 15368–15371.
[26] R.S. Khnayzer, V.S. Thoi, M. Nippe, A.E. King, J.W. Jurss, K.A. El Roz, J.R. Long, C.J. Chang, F.N. Castellano, Energy Environ. Sci. 7 (2014) 1477–1488.
[27] J. Zhao, S. Ji, W. Wu, W. Wu, H. Guo, J. Sun, H. Sun, Y. Liu, Q. Li, L. Huang, RSC Adv. 2 (2012) 1712–1728.
[28] E. Deponti, M. Natali, Dalton Trans. 45 (2016) 9136–9147.
[29] C.V. Krishnan, N. Sutin, J. Am. Chem. Soc. 103 (1981) 2141–2142.
[30] G.B. Bodedla, L. Li, Y. Che, Y. Jiang, J. Huang, J. Zhao, X. Zhu, Chem. Commun. 54 (2018) 11614–11617.
[31] Y. Tsuji, K. Yamamoto, K. Yamauchi, K. Sakai, Angew. Chem. Int. Ed. 57 (2018) 208–212.
[32] I. Ghosh, R.S. Shaikh, B. König, Angew. Chem. Int. Ed. 129 (2017) 8664–8669.
[33] S. Berardi, S. Drouet, L. Francas, C. Gimbert-Surinach, M. Guttentag, C. Richmond, T. Stoll, Chem. Soc. Rev. 43 (2014) 7501–7519.
[34] M.D. Karkas, O. Verho, E.V. Johnston, B. Akermark, Chem. Rev. 114 (2014) 11863–12001.
[35] V. Balzani, A. Credi, M. Venturi, ChemSusChem 1 (2008) 26–58.
[36] W. Wu, S. Ji, W. Wu, J. Shao, H. Guo, T.D. James, J. Zhao, Chem. Eur. J. 18 (2012) 4953–4964.
[37] L. Chen, S. Sun, J. Li, Z. Fang, Inorg. Chim. Acta 446 (2016) 24–31.
[38] A.K. Singh, G. Saxena, M. Sahabjada, Arshad, Spectrochim. Acta, Part A 180 (2017) 97–104.
[39] Y. Ueno, J. Jose, A. Loudet, C. Perez-Bolivar, P. Anzenbacher Jr., K. Burgess, J. Am. Chem. Soc. 133 (2011) 51–55.
[40] M.D. Yilmaz, O.A. Bozdemir, E.U. Akkaya, Org. Lett. 8 (2006) 2871–2873.
[41] R.S. Khnayzer, B.S. Olaiya, K.A. El Roz, F.N. Castellano, ChemPlusChem 81 (2016) 1090–1097.
[42] C. Creutz, N. Sutin, J. Am. Chem. Soc. 98 (1976) 6384–6385.
[43] L.A. Kelly, M.A.J. Rodgers, J. Phys. Chem. 98 (1994) 6377–6385.
[44] S. Guo, L. Xu, K. Xu, J. Zhao, B. Kucukoz, A. Karatay, H.G. Yaglioglu, M. Hayvali, A. Elmali, Chem. Sci. 6 (2015) 3724–3737.
[45] M.E. El-Khouly, A.N. Amin, M.E. Zandler, S. Fukuzumi, F. D'Souza, Chem. Eur. J. 18 (2012) 5239–5247.
[46] R. Ziessel, B.D. Allen, D.B. Rewinska, A. Harriman, Chem. Eur. J. 15 (2009) 7382–7393.